04

Experimental determination of the indicatrix of scattered laser radiation from plasma at an advanced multi-channel high-power laser setup

© L.M. Lavrov, E.V. Pozdnyakov, V.M. Yamshchikov, A.S. Mokeev, M.A. Yamshchikova

Russian Federal Nuclear Center, All-Russia Research Institute of Experimental Physics, Sarov, Russia
E-mail: feynman94@yandex.ru

Received August 18, 2025
Revised October 9, 2025
Accepted November 5, 2025

The indicatrix of radiation scattered by laser plasma was determined at an advanced multi-channel high-power laser setup. Planar targets were irradiated with a laser pulse with a wavelength of 532 nm, an energy of 2.1−3.65 kJ, and a duration of 3−5 ns. The indicatrix was determined at angles of 2–90° to the normal vector to the target surface. It was demonstrated that side scattering (in the region of angles greater than 45°) is lacking at an intensity $\leq 2.6 \cdot 10^{14}$ W/cm^2; instead, backscattering in the form of a double cone was recorded. Pronounced side scattering directed perpendicular to the polarization plane emerged at an intensity $\geq 3.4 \cdot 10^{14}$ W/cm^2.

Keywords: scattered radiation indicatrix, laser plasma, photo paper.

DOI: 10.21883/0000000000

Despite the recent breakthrough in laser thermonuclear fusion (LTF) [1,2], the presence of nonlinear processes in laser-plasma interactions is regarded as one of the factors preventing efficient ignition of a thermonuclear reaction in LTF [3,4]. For example, stimulated Brillouin−Mandelstam scattering (SBMS) and stimulated Raman scattering (SRS) [5] lead to loss of laser energy and plasma cooling.

Theoretical studies of nonlinear processes in laser plasmas conducted in the 1970−1990s [6] were centered largely on stimulated Raman backscattering (SRBS) and SBMS, which are directed back into focusing optics. The number of studies focused on radiation scattering in side directions with angles of deviation from the normal to the target surface exceeding 45° was limited for the following reasons: (1) it is difficult to obtain an experimental directional pattern within a wide range of angles, since this requires the use of a large number of radiation receivers, imposing additional requirements on the camera design and on measurement techniques [4]; (2) side scattering was observed at high-power laser setups that have the capacity to raise the value of product I_0L above 10^{17} W·μm/cm^2 (I_0 is the threshold value of laser flux [W/cm^2] and L is the characteristic plasma size [μm]) [7,8]. Only modern high-energy facilities used in LTF experiments provide the required power density ($10^{14}-10^{15}$ W/cm^2) coupled with a sufficiently large spot size (upward of 500 μm) and nanosecond duration. Such conditions may be established in experiments at an advanced multi-channel high-power laser setup [9].

An example illustrating the state of research on side scattering, which was carried out back in the 1980s, is provided by [10]. The authors of this study used ~ 10 photodetectors, which is insufficient to obtain in-depth information regarding the scattered radiation indicatrix with high resolution within a wide range of angles. Transverse scattering in the direction of angles close to 90° was also not reported due to the lack of photodetectors in this angle region. The recorded scattered light energy was ~ 1% of the laser energy, while the corresponding value in the present work is ~ 10%.

The propagation of radiation from plasma in the region of angles of 75−90°, which was called transverse scattering, has been observed experimentally for the first time in [11]. Transverse scattering, which was called tangential side scatter in foreign literature, was later investigated in experiments with direct irradiation of a planar target with one or several beams [4,7].

It has been confirmed in recent years [12] that side scattering is observed in experiments at NIF due to the large laser focal spot size and high laser intensity. Therefore, a more thorough understanding of this process, which causes additional energy loss and leads to plasma cooling, is needed. New diagnostic methods, which allow one to perform measurements at various observation angles up to 90° [4], are currently being introduced into the research arsenal. However, a full directional pattern of scattered radiation within a wide range of angles has not been obtained yet.

The role of laser radiation (LR) polarization in the formation of directional pattern of scattered radiation remains virtually undiscussed in the literature. It was noted in [4] that side scattering is directed perpendicular to the plane of polarization, but no targeted studies into the role of polarization in the process of LR scattering have been conducted. The mutual influence of the direction of polarization vectors of two laser beams focused into the same spot on a target on the amount of energy scattered into focusing optics was investigated experimentally in [13].

The aim of the present study is to determine the indicatrix of radiation scattered by laser plasma within a wide range

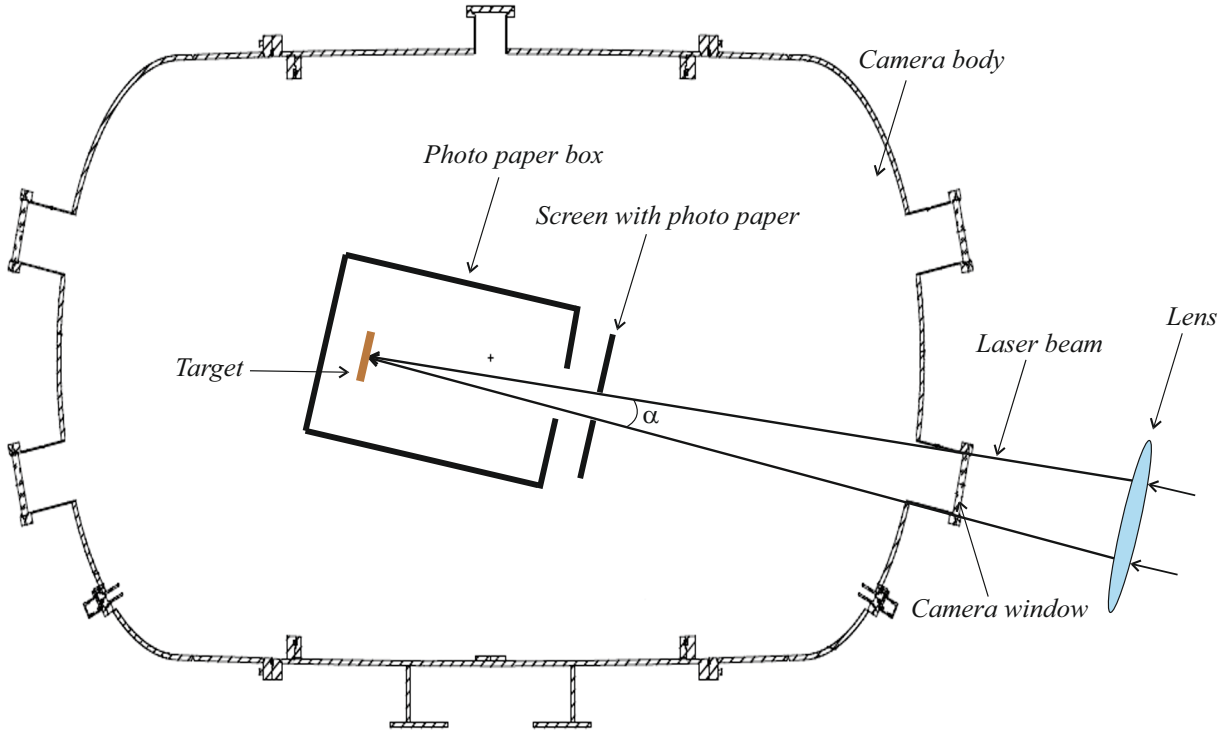

Figure 1. Diagram of the experiment.

of angles and estimate the energy losses due to scattering using the technique detailed in [14].

Experiments on scattering of laser radiation from plasma were carried out at an advanced multi-channel high-power laser setup [9] using a single laser channel. The radiation wavelength, pulse energy, and pulse duration were $\lambda = 532\,\text{nm}$, $E = 2.1-3.65\,\text{kJ}$, and $\tau = 3-5\,\text{ns}$, respectively. The focal spot size was controlled with a pinhole camera and was $\sim 500\,\mu\text{m}$. A planar copper target positioned perpendicular to incident radiation was used. Its length, width, and thickness were 20, 17, and 2 mm, respectively.

Calibrated photo paper (PP) [14] was used to plot the spatial pattern of scattering of radiation from plasma within a solid angle of $\sim 2\pi$. It provides an opportunity to detect radiation within a wide range of frequencies from UV to IR at a threshold energy density of $0.05\,\text{J/cm}^2$, which is what is required to form a visible burn.

The procedure for calibrating PP sensitivity was detailed in [14], where the dynamic range of energy density recording was demonstrated to be 10 at a radiation duration of ~ 1 ns.

The optical diagram of experiments on nonlinear scattering is shown in Fig. 1. LR was focused onto the target by a lens with focal length $f = 7\,\text{m}$. The laser beam entering the lens has a size of 330×330 mm. The residual gas pressure in the chamber did not exceed 10^{-5} mm Hg.

Scattered radiation was detected within the range of angles from 12 to 90° by PP positioned on the inner surface of a cylindrical box with the following internal dimensions: diameter, 34 cm; length, 45 cm. The target inside the box was positioned on its axis at a distance of 5 cm from the rear end.

A screen with PP located at a distance of 84 cm from the target was used to record scattered radiation within the range of angles from 2 to 12°.

At a laser flux I of $2.6 \cdot 10^{14}\,\text{W/cm}^2$, no visible burns were found on photo paper on the side wall of the cylindrical box; this suggests that transverse scattering was lacking. At the same time (see Fig. 2), severe burns were seen on PP on the screen positioned opposite the target at a distance of 84 cm from it.

Intense transverse scattering emerged at laser fluxes above $I = 3.4 \cdot 10^{14}\,\text{W/cm}^2$. In this case, the product of I and the characteristic size of plasma formation ($500\,\mu\text{m}$) is $\sim 10^{17}\,\text{W}\cdot\mu\text{m/cm}^2$ [7,8]. The laser beam passed through a round hole 60 mm in diameter or a 50×50 mm square hole in the center of the screen. This hole is covered with black paper in the photographic images of burns shown in Figs 2, *a–c*.

Figure 2, *d* presents the photographic images of burns on photo paper positioned on the end wall of the box and on the screen (combined view), as well as inside the box (unfolded side surface of the cylinder). The conditions of these experiments enabled transverse scattering.

The photographic images of burns demonstrate that the radiation scattering indicatrix has several preferential directions.

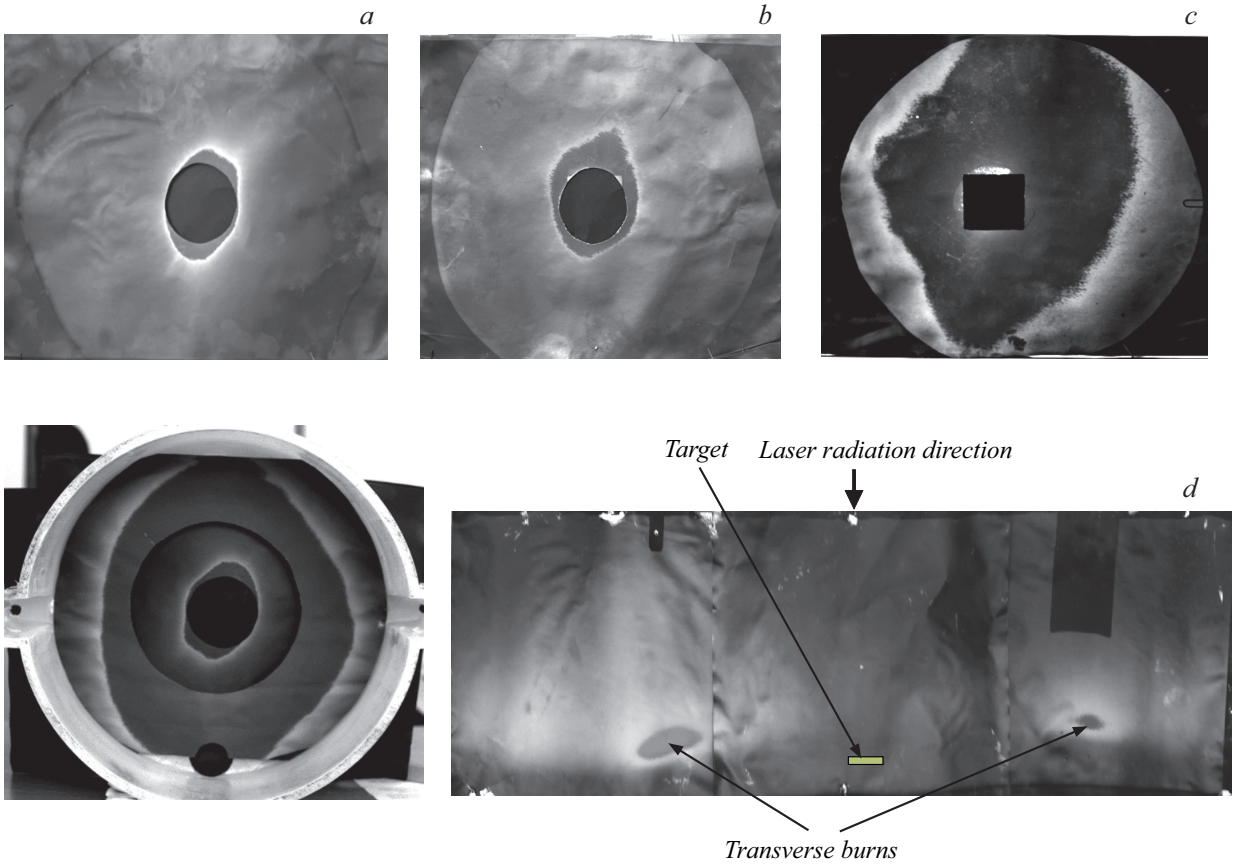

Figure 2. Burns on photo paper: $a-c$ — located on the screen (at a distance of 84 cm from the target); d — located on the side of focusing optics (at the end of the box at a distance of 40 cm from the target and on the screen at a distance of 84 cm from the target) and on the side surface of the cylinder (unfold). a — $E = 2.1$ kJ, $\tau = 4.1$ ns, $I = 2.6 \cdot 10^{14}$ W/cm^2, no transverse scattering; b — $E = 3.2$ kJ, $\tau = 4.3$ ns, $I = 3.8 \cdot 10^{14}$ W/cm^2, transverse scattering is present; c — $E = 3.65$ kJ, $\tau = 5.4$ ns, $I = 3.4 \cdot 10^{14}$ W/cm^2, transverse scattering is present; d — $I = 3.4 \cdot 10^{14}$ W/cm^2, transverse scattering is present.

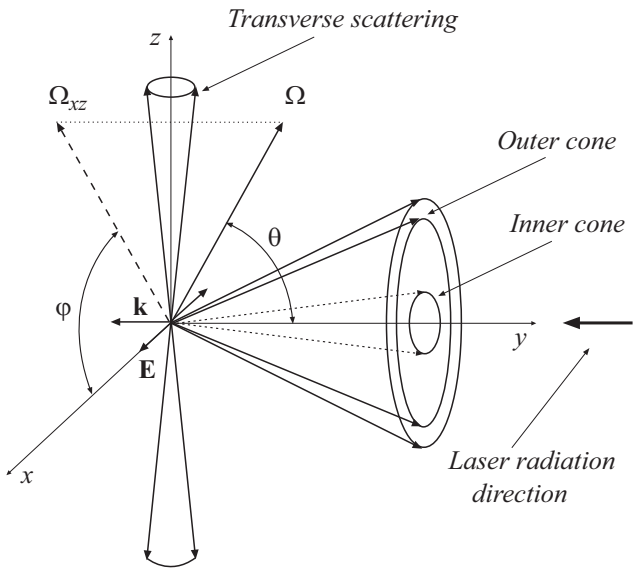

Figure 3. Directional pattern of scattered radiation.

1. The directional pattern of radiation scattered toward the focusing optics has the form of two cones with apex angles measured from the normal to the target surface. The inner cone angle increases from 6 to 20° with an increase in laser radiation energy from 2.1 to 3.65 kJ. At the same time, the outer cone angle varies little with laser radiation energy, and its angular size is $\sim 30-40°$.

2. Intense burns in the direction perpendicular to the laser beam and the polarization vector (transverse scattering) emerge at LR intensities above $3.4 \cdot 10^{14}$ W/cm^2 (see Fig. 2, *d*).

A schematic directional pattern was plotted based on the experimentally obtained PP burn pattern. This diagram is presented in Fig. 3,

where **k** is the wave vector of laser radiation, **E** is the electric field vector of a laser wave oscillating linearly in plane xy, **Ω** is the propagation direction vector for scattered radiation, $\mathbf{\Omega}_{xz}$ is the projection of vector **Ω** onto plane xz, θ (zenith angle) is the angle between axis y and vector **Ω**, and φ (azimuth angle) is the angle between $\mathbf{\Omega}_{xz}$ and axis x. The experimental data [15] demonstrate that the direction of transverse scattering is not related to the beam geometry in

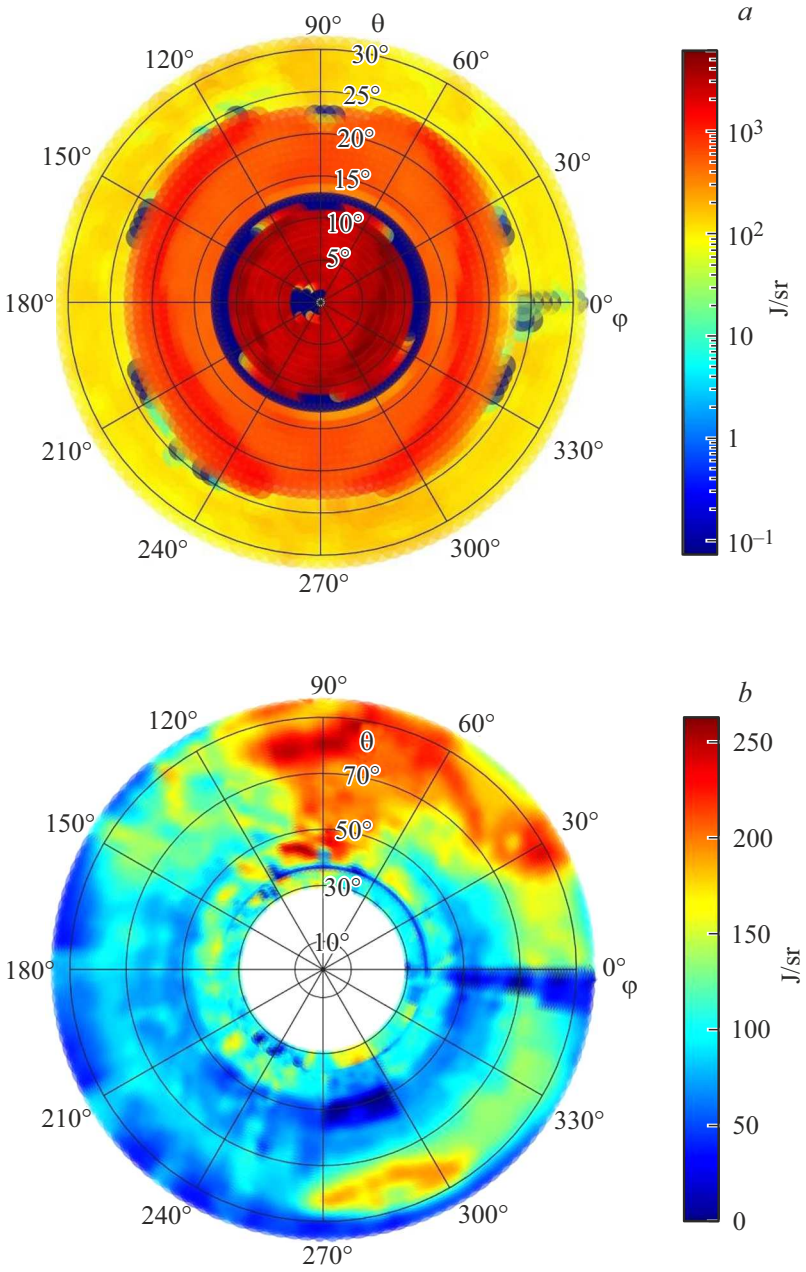

Figure 4. Indicatrix of radiation scattered by laser plasma (in J/sr), $I = 3.4 \cdot 10^{14}$ W/cm^2. *a* — Angle θ ranges from 0 to 30°; *b* — θ ranges from 30 to 90°.

the focal region; in all cases, it is perpendicular to the plane of polarization.

Analyzing the burns on photo paper and the results of its sensitivity calibration, which were presented in [14], one may determine the amount of energy dissipated in different directions (indicatrix). Figure 4 shows the indicatrix obtained using a laser pulse with $E = 3.65$ kJ and $\tau = 5.4$ ns. Angle θ is measured from the normal vector to the target surface (zenith angle), while φ is the azimuth angle. The indicatrix is shown in Figs. 4, *a* and *b*.

Two cones are seen clearly in Fig. 4, *a*. This is consistent with the burn pattern in Fig. 2, *d*. The first cone lies within the range of angles θ varying from 2 to 11° (the cone angle varies from 4 to 22°). The second cone lies within the range of angles varying from 13 to 23° (the cone angle varies from 26 to 46°).

Two preferential directions of radiation propagation corresponding to transverse scattering are seen in Fig. 4, *b*. The first direction corresponds to angle $\varphi = 90°$ and angles θ varying from 45 to 90°. The second direction is almost diametrically opposite to the first one and corresponds to angle $\varphi = 285°$ and angle $\theta = 80°$. This is consistent with the burn pattern in Fig. 2, *d*.

The obtained indicatrix was used to determine the values of energy scattered in different directions and within a solid angle of 2π: (1) 325 J were scattered into the inner cone;

(2) 233 J were scattered into the outer cone; (3) 502 J were scattered to the side directions; (4) 1060 J (29 % of the laser pulse energy) were scattered within a solid angle of 2π. The energy entering the focusing optics was neglected in this case. The determined values of losses due to scattering of laser radiation agree well with the results reported in [11,15–18].

The transverse scattering pattern from [4] agrees qualitatively and quantitatively with the pattern reported here. However, it should be noted that the indicatrix obtained in [4] featured no radiation scattering in the form of cones.

Data on the mechanisms of occurrence and formation of side and transverse scattering are relatively scarce in current scientific literature, which makes it impossible to draw an unambiguous conclusion regarding the obtained indicatrix. That said, we note theoretical study [19], where the factors affecting the process of formation of SRS at large angles ($45 < \theta \leq 90^\circ$) were determined by calculation. It was demonstrated that such scattering is associated with periodic modulation of electron density in rarefied plasma caused by ponderomotive forces. A detailed pattern of scattering within a wide range of angles is needed to verify the proposed model.

A directional pattern of radiation scattered from laser plasma has been obtained for the first time with a high spatial resolution and within a wide range of solid angles ($\sim 2\pi$). A scattering indicatrix was obtained using the pattern of burns on photo paper and the results of its sensitivity calibration. It was demonstrated that a significant part of scattered energy is directed opposite in the form of two cones and perpendicular to the plane of polarization. The obtained indicatrix revealed that 29 % of laser energy are converted into scattered radiation energy.

The laser radiation intensity threshold corresponding to the emergence of noticeable transverse scattering in the region of angles of $75-90^\circ$ in the direction perpendicular to the plane of polarization was determined to be $\sim 3 \cdot 10^{14}$ W/cm^2.

Conflict of interest

The authors declare that they have no conflict of interest.

References

[1] H. Abu-Shawareb and Indirect Drive ICF Collaboration, Phys. Rev. Lett., **129** (7), 075001 (2022). DOI: 10.1103/PhysRevLett.129.075001
[2] D. Kramer, Phys. Today, Iss. 2, 1213a (2022). DOI: 10.1063/PT.6.2.20221213a
[3] R.L. Berger, C.A. Thomas, K.L. Baker, D.T. Casey, Phys. Plasmas, **26** (1), 012709 (2019). DOI: 10.1063/1.5079234
[4] K. Glize, X. Zhao, Y.H. Zhang, C.W. Lian, S. Tan, F.Y. Wu, C.Z. Xiao, R. Yan, Z. Zhang, X.H. Yuan, J. Zhang, Phys. Plasmas, **30** (12), 122706 (2023). DOI: 10.1063/5.0180607
[5] Y.R. Shen. *The Principles of Nonlinear Optics* (Wiley, 1984).
[6] V.T. Tikhonchuk, Sov. J. Quantum Electron., **21** (2), 133 (1991).].
[7] G. Cristoforetti, L. Antonelli, S. Atzeni, F. Baffigi, F. Barbato, D. Batani, G. Boutoux, A. Colaitis, J. Dostál, R. Dudzak, L. Juha, P. Koester, A. Marocchino, D. Mancelli, P. Nicolaï, O. Renner, J. Santos, A. Schiavi, M. Škorić, M. Šmíd, P. Straka, L. Gizzi, Phys. Plasmas, **25** (1), 012702 (2018). DOI: 10.1063/1.5006021
[8] M.J. Rosenberg, A.A. Solodov, J.F. Myatt, W. Seka, P. Michel, M. Hohenberger, R.W. Short, R. Epstein, S.P. Regan, E.M. Campbell, T. Chapman, C. Goyon, J.E. Ralph, M.A. Barrios, J.D. Moody, J.W. Bates, Phys. Rev. Lett., **120** (5), 055001 (2018). DOI: 10.1103/PhysRevLett.120.055001
[9] S.A. Belkov, B.G. Zimalin, P.Yu. Kruglov, A.O. Lipatov, A.N. Manachinskii, A.V. Yakhlov, Bull. Lebedev Phys. Inst., **51** (2), 165 (2024). DOI: 10.3103/S106833562460058X.
[10] R.P. Drake, R.E. Turner, B.F. Lasinski, K.G. Estabrook, E.M. Campbell, C.L. Wang, D.W. Phillion, E.A. Williams, W.L. Kruer, Phys. Rev. Lett., **53** (18), 1739 (1984). DOI: 10.1103/PhysRevLett.53.1739
[11] L.M. Lavrov, A.V. Bessarab, D.I. Martsovenko, F.A. Starikov, A.A. Andreev, K.Yu. Platonov, Opt. Spectrosc., **111** (2), 184 (2011). DOI: 10.1134/S0030400X11080200.
[12] M.J. Rosenberg, A.A. Solodov, J.F. Myatt, S. Hironaka, J. Sivajeyan, R.K. Follett, T. Filkins, A.V. Maximov, C. Ren, S. Cao, P. Michel, M.S. Wei, J.P. Palastro, R.H.H. Scott, K. Glize, S.P. Reganl, Phys. Plasmas, **30** (4), 042710 (2023). DOI: 10.1063/5.0135603
[13] I. Barth, N.J. Fisch, Phys. Plasmas, **23** (10), 102106 (2016). DOI: 10.1063/1.4964291
[14] L.M. Lavrov, E.V. Pozdnyakov, E.A. Ul'mov, V.M. Yamshchikov, M.A. Yamshchikova, Instrum. Exp. Tech., **66** (6), 926 (2023). DOI: 10.1134/S0020441223050329.
[15] L.M. Lavrov, E.V. Pozdnyakov, V.M. Yamshchikov, M.A. Yamshchikova, Tech. Phys., **70** (4), 642 (2025). DOI: 10.61011/TP.2025.04.61204.136-24.
[16] R. Sigel, J. de Phys. C6, **38**, C6-35 (1977). DOI: 10.1051/jphyscol:1977605
[17] Yu.Yu. Protasov, V.V. Khristoforov, Vestn. MGTU N.E. Baumana. Ser. Estestv. Nauki, **30** (3), 37 (2008) (in Russian).
[18] D.A. Borisevichus, V.V. Zabrodskii, S.G. Kalmykov, M.E. Sasin, R.P. Seisyan, Tech. Phys. Lett., **43** (1), 67 (2017). DOI: 10.1134/S1063785017010060.
[19] Z.M. Huang, Qing Wang, R.J. Cheng, X.X. Li, S.Y. Lv, D.J. Liu, Z.Y. Xu, S.T. Zhang, Z.J. Chen, Qiang Wang, C.Z. Xiao, Z.J. Liu, L.H. Cao, C.Y. Zheng, X.T. He, Matter Radiat. Extrem., **10** (5), 057403 (2025). DOI: 10.1063/5.0278141

Translated by D.Safin